International Journal of Engineering Trends and Technology
ISSN: 2231 – 5381 / https://doi.org/10.14445/22315381/IJETT-V70I8P203
Volume 70 Issue 8, 26-41, August 2022

Original Article

GA-Based POD and GADC-Based Voltage Regulator for IPFC to Dampen Low-Frequency Oscillations

D. Obulesu[1], Manjunatha S C [2]

[1]*Department of EEE, CVR College of Engineering, Telangana, Hyderabad, India.*
[2] *SJM Institute of Technology / EEE Department, Chitradurga, Karnataka, India*

dakkaobulesh@gmail.com

Received: 25 May 2022 Revised: 28 June 2022 Accepted: 11 July 2022 Published: 09 August 2022

Abstract *- The new GAPOD-and GADC-based voltage controllers for the suppression of LF oscillations for the IPFC in the integrated-connected power systems are proposed in this research work to dampen the fluctuations and improve the quality of power (power quality - PQ). The developed controller was compared with the PSOMSF-based DC type of voltage controller, the GAMSF-based DC type of voltage controller and the conventional type of IPFC controllers in an MMPS under various operating parameters. The findings obtained in this work indicate that the GAPOD-GADC-based voltage regulators are quite successful in operation. They provide good output in the face of changing operational conditions and severe load disruptions.*

Keywords *- IPFC, PSOMSF-based DC type of voltage controller, GAMSF-based DC type of voltage controller, MMPS(multi-machine power system).*

1. Introduction

The authors in [1] worked on modelling a SMIB network, which was incorporated using an IPFC and an SVC. A power system stabilising (PSS) unit without the FACT-based controlling component could be developed, created, and implemented. A synchronised control configuration of IPFC and SVC without the PSS could be carried out after choosing the most appropriate IPFC control signal utilising the residual-based theory. In the absence of PSS, the IPFC- and SVC-based dynamic controllers could be used to dampen out the LF fluctuations or the distortions. They then demonstrated that the PSS controller outperformed other controllers in terms of enhancing the dynamic stability of the power grid. Furthermore, in the absence of the PSS system, the IPFC and SVC controllers behaved admirably with good performance criteria and achievements. The PSS controller outperformed other controllers to enhance the dynamic stability, and the results of IPFC and SVC controllers proved adequate in the absence of PSS.

In the research paper discussed in [2], the authors investigated IPFC effects on an advanced FACTS controlling system for dampening the LF PS oscillations using additional controlling circuitry. A revised and linearised PH model for an IPFC-installed SMIB system was set up to implement this dampening process. The POD controlling device was remodelled and tested to produce satisfactory results. It investigated the effects of the dampening controlling device on the power system network, subjected to large fluctuations in load situations (light and heavy loads) and the parameters of the system's network with T-lines. Results of dynamic simulations have demonstrated that under large changes in the loading condition and device variables, the dampening controllers that modulate the controlled waveform parameter m_2 give more dynamic efficiency during the operating conditions.

The authors in [3] developed a nonlinear model of FACTS-type IPFC equipped with SMIB in addition to the Heffron Philips model. The optimal variables in the IPFC controlling circuitry were determined using the PSO algorithm based on two fitness functions. Moreover, the candidate signal for the dampening of LF oscillations of IPFC input signals was selected based on controllability indices that consider the best signal is having a high index (Δm_2) and the worst signal to have the lowest one ($\Delta\delta_1$). The SMIB incorporated with the IPFC damping controller was investigated in a wide range of operating zones through eigenvalue analysis and simulations in the nonlinear mode to prove the robust property and effectiveness of damping controller settings.

The researchers in [4]performed extensive work on establishing the linearised P–H model of an IPFC-mounted power system. The P–H damping controllers were configured to dampen the LF oscillations in a power system network, considering four alternate damping controllers based on the IPFC. Simulation findings of Matlab/Simulink showed that the signals ml and m_2 had a greater effect on the damping oscillations, and the δ_1 signal andδ_2-dependent controllers had a lower effect on oscillation damping.

The researchers in paper [5] worked on designing additional controllers based on fuzzy logics (FL) mounted with IPFC for dampening LF oscillations and harmonics. The qualitative efficacy of control signals (m_1, m_2, δ_1, δ_2) of the IPFC in dampening LF harmonics was tested thoroughly to arrive at very good results. In conjunction with the power oscillation dampening (POD) controlling unit, the power system stabilising (PSS) unit, and the fuzzy logic controlling (FLC) unit, the linearised power system model of the SMIB framework for evaluating the output comparisons of the IPFC has been considered in this paper.

2. Controller Designs for IPFC-Based POD

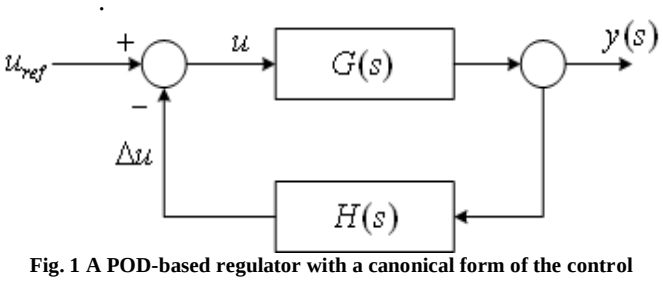

Fig. 1 A POD-based regulator with a canonical form of the control system

A mathematical model could be used to define changes in an eigenvalue problem *i*. The objective of the FACTS damping regulations is to boost the damping ratio of the chosen oscillatory phase; that is, to move the real part of the eigenvalue *I* to the left half complex plane, $\Delta\lambda i$ must be a really small number. The displacement of the eigenvector value after the FACTS damping control behaviour is shown in Fig. 3, and the mathematical model under such conditions is given by

$$\Delta\lambda_i = R_1 \times K \times H_1 \times \lambda_1$$

With the same feedback loop gain, a larger residue would result in a larger shift of the corresponding oscillatory mode, as shown in the model equation. Thus, for the considered excitation mode, the best feedback signal for the FACTS damping controller would be the one with the maximum PFE constant. The same can be said about the best location for the POD regulator, which also happens to be the best location for the FACTS unit. The compensation angle ϕ_{comp} needed to transfer the eigenvalue directly to the left parallel to the real axis is shown in Fig. 3

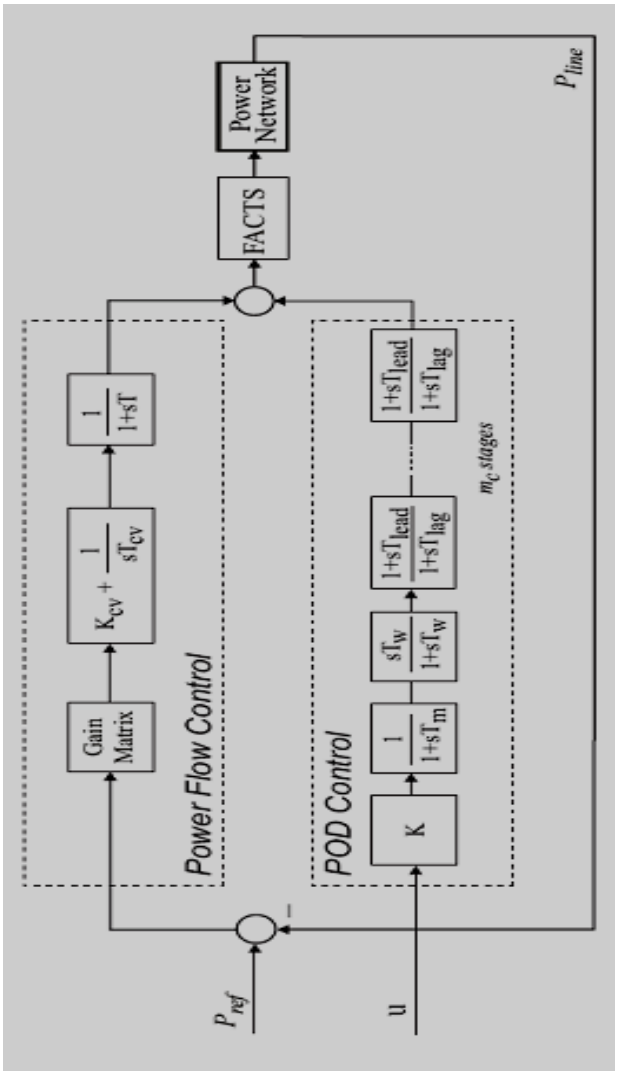

Fig. 2 Controlling structure of the FACTS-based controlling circuitry used

The lead and lag time constants are given by T_{lead} and T_{lag}, a slag function, and the parameters T_{lead} and T_{lag} are determined by the following equations:

$$T_{lag} = \frac{1}{\omega_i \sqrt{\alpha_c}}$$

$$\mathrm{T}_{lead} = \alpha_c T_{lag}$$

Where (R_i) denotes the phase angle of the residue R_i , ω_i is the frequency of the mode of fluctuations in radians per second and m_c is the number of compensation stages, considered as m_c = 2. The controller gain *K* is computed as a function of the desired eigenvalues λ_i location, according to the equation mentioned above

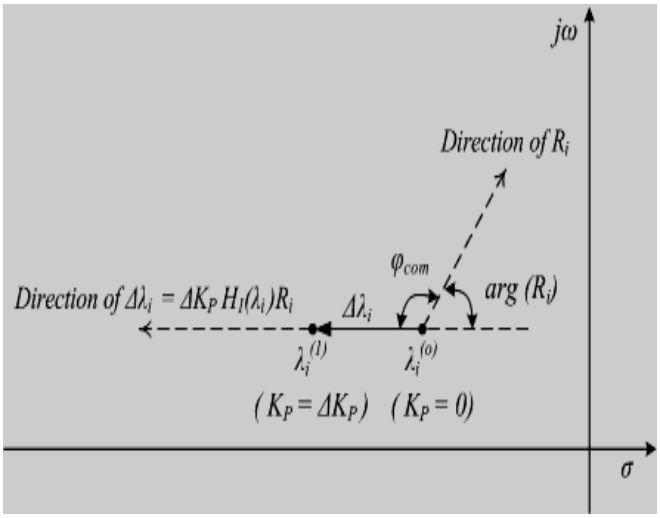

Fig. 3 Shifting of the eigen parametric values for the POD-based controller

$$K = \left| \frac{\lambda_{i,\text{des}} - \lambda_i}{R_i H(\lambda_i)} \right|$$

3. Analysis and Simulations of the Developed Controller in MMIB

The multi-machine electrical power system equipped with IPFC, as displayed in Fig. 4, utilised for research purposes to dampen out harmonic oscillations and improve the PQ, comprises the following blocks: an ET, a BT, two3ϕ GTO-dependent VSCs and a DC-linked condenser. The standard IEEE 6-generator 30-bus system is considered for the analysis. To investigate the possibilities of the damping of LF perturbations in an MMIB-based power system, we implemented the two developed controllers to analyse the SMIB system, and the effectiveness of the controllers was studied.

Here, for the analysis, we are recording the time response of Δδ (rotor angle deviations), the time response of ΔPe (electrical power deviations) and the time response of Δω (rotor speed deviations). From the optimal scheduling, we consider bus 2 as our reference bus, and the IPFC controller is placed between lines 2–5 and 2–6. The controllers already developed in the first part were imposed on the IPFC. These are the conventional IPFC controller, the genetic algorithm-based multistage fuzzy – GAMSF-based DC type of voltage controller, the PSOMSF-based DC type of voltage controller, the GA-based POD and the GADC-based voltage-dependent controllers.

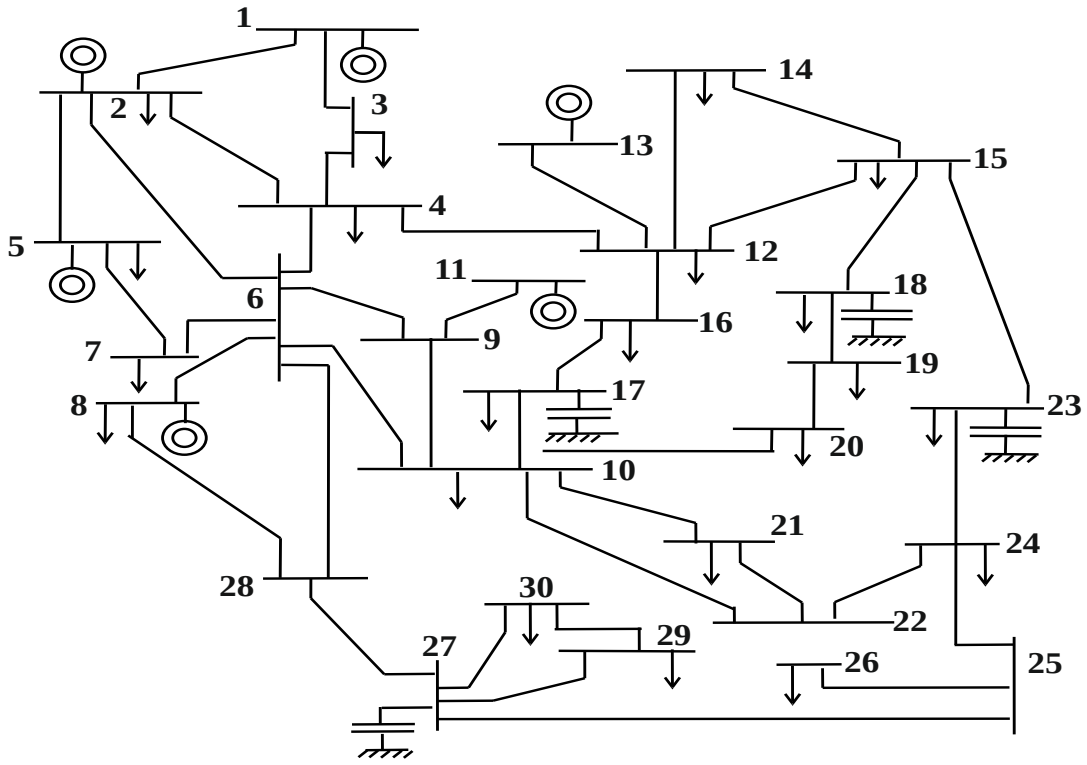

Fig. 4 The standard IEEE 6-generator 30-bus system equipped with IPFC

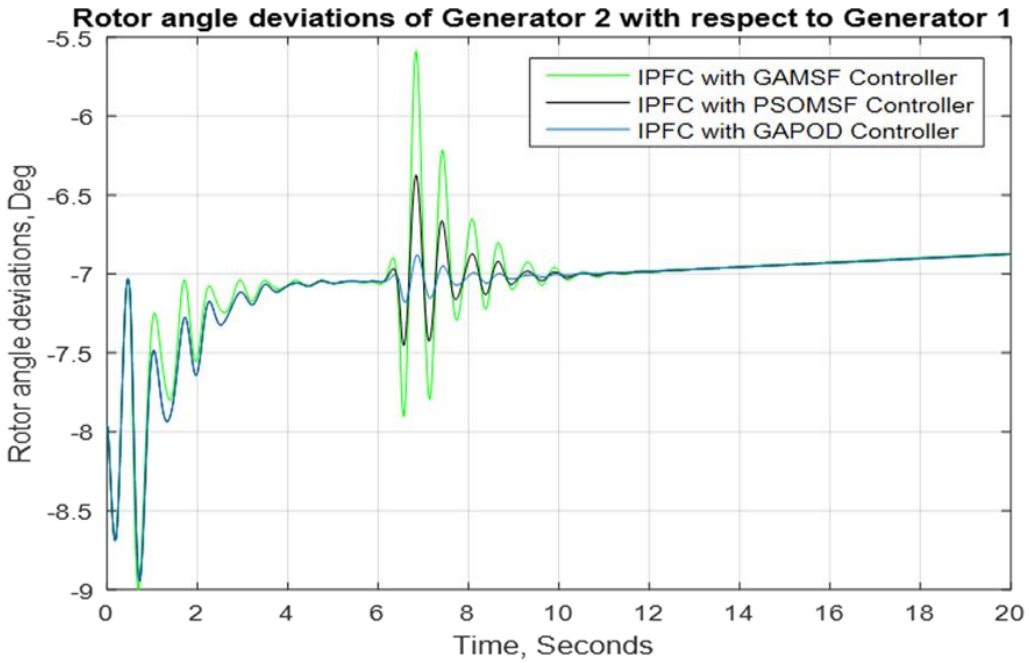

Fig 5. TR of the deviation in the rotor's angle of machine no. 2 concerning machine or generator no. 1 utilising the conventional/traditional type of controller, the GAMSF-based controller, the PSO-MSF-based DC type of voltage controller and the GAPOD-based DC type of voltage regulator at operating points 1 and 2 in the MMPS

Fig. 5 shows the time responses of the deviation in the rotor's angle of machine no. 2 concerning machine or generator no. 1 using the conventional/traditional type of controller, the GAMSF-based controller, the PSO-MSF-based DC type of voltage controller and the GAPOD-based DC type of voltage regulator at the first and second points of operation in the MMPS. In the simulated results shown, the first part, from 0 to 6 seconds, is for operating point 1 and the second part, from 6 to 12 seconds, is for operating point 2. In both cases, the GAPOD-based DC type of voltage regulator provides effective damping compared to conventional controllers.

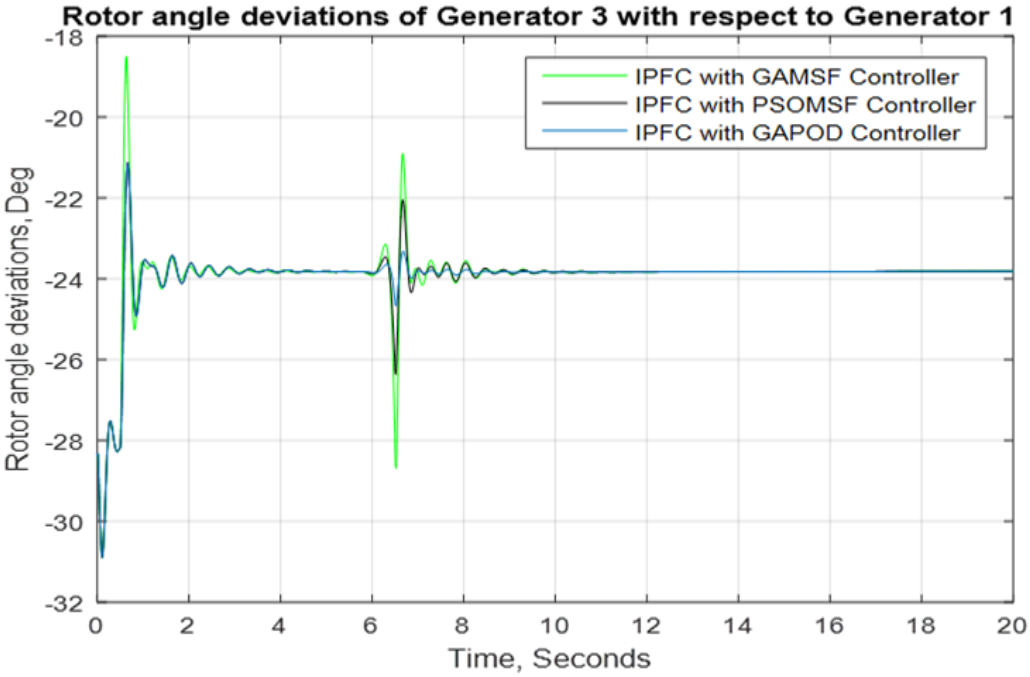

Fig. 6 TR of the deviation in the rotor's angle of the machine no. 3 concerning the machine or generator no.1 utilising the conventional/traditional type of controller, the GAMSF-based controller, the PSO-MSF-based DC type of voltage controller and the GAPOD-based DC type of voltage regulator at operating points1 and 2 in the MMPS

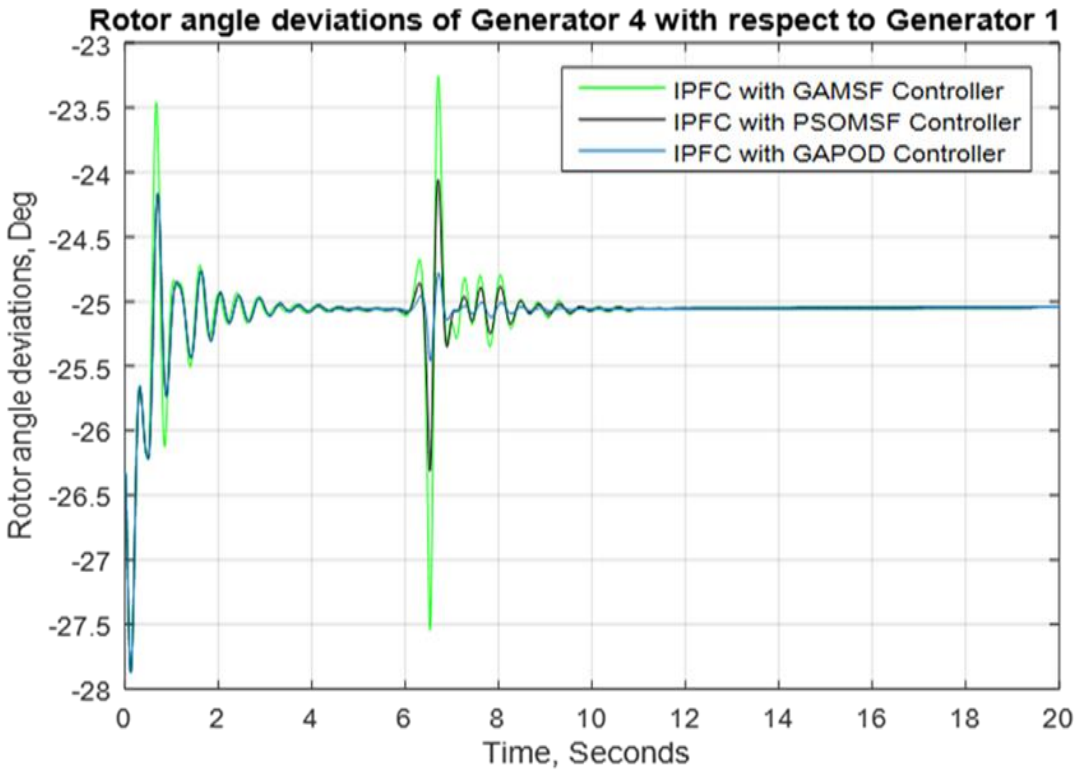

Fig. 7 TR of the deviation in the rotor's angle of machine no.4 concerning the machine or generator no.1 utilising the conventional/traditional type of controller, the GAMSF-based controller, the PSO-MSF-based DC type of voltage controller and the GAPOD-based DC type of voltage regulator at operating points 1 and 2 in the MMPS

Fig. 6 shows the time-responses of the deviation in the rotor's angle of machine no.3 concerning the machine or generator no.1 using the conventional/traditional type of controller, the GAMSF-based controller, the PSO-MSF-based DC type of voltage controller and the GAPOD-based DC type of voltage regulator at the first and second points of operation in the MMPS. In the simulated results shown, the first part, from 0 to 6 seconds, is for operating point 1 and the second part, from 6 to 12 seconds, is for operating point 2. In both cases, the GAPOD-based DC type of voltage regulator provides effective damping compared to conventional controllers.

Fig 7 shows the time-responses of the deviation in the rotor's angle of machine no. 4 concerning machine or generator no. 1 using the conventional/traditional type of controller, the GAMSF-based controller, the PSO-MSF-based DC type of voltage controller and the GAPOD-based DC type of voltage regulator at the first and second points of operation in the MMPS. In the simulated results shown, the first part, from 0 to 6 seconds, is for operating point 1 and the second part, from 6 to 12 seconds, is for operating point 2. In both cases, the GAPOD-based DC type of voltage regulator provides effective damping compared to conventional controllers.

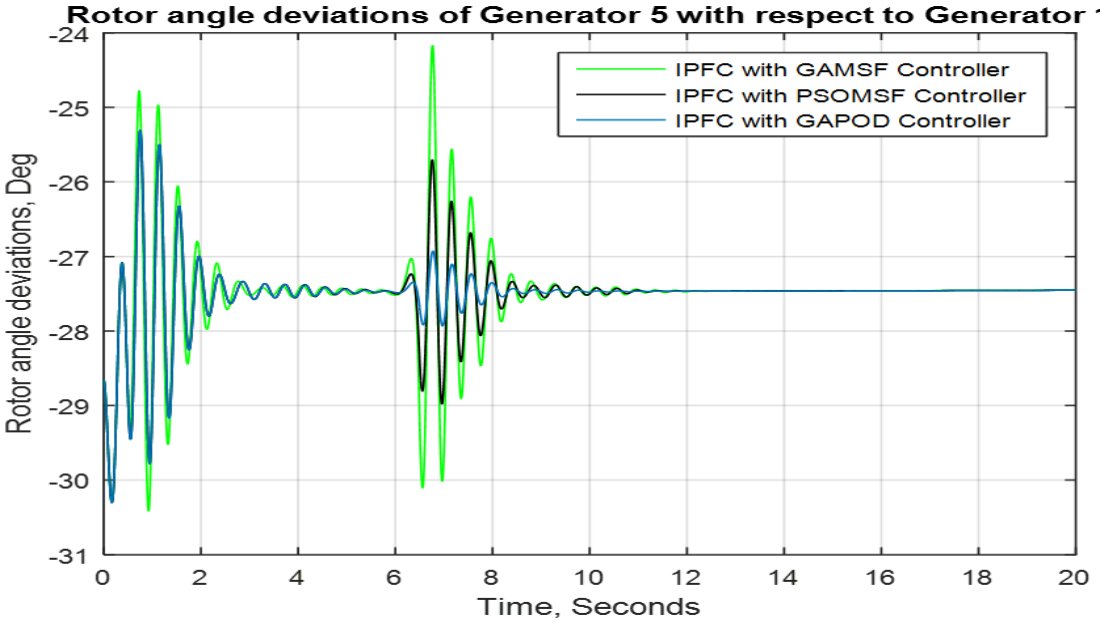

Fig. 8 TR of the deviation in the rotor's angle of machine no.5 concerning the machine or generator no.1 utilising the conventional/traditional type of controller, the GAMSF-based controller, the PSO-MSF-based DC type of voltage controller and the GAPOD-based DC type of voltage regulator at operating points 1 and 2 in the MMPS.

Fig. 8 shows the time-responses of the deviation in the rotor's angle of machine no.5 concerning machine or generator no.1 using the conventional/traditional type of controller, the GAMSF-based controller, the PSO-MSF-based DC type of voltage controller and the GAPOD-based DC type of voltage regulator at the first and second points of operation in the MMPS. In the simulated results shown, the first part, from 0 to 6 seconds, is for operating point 1 and the second part, from 6 to 12 seconds, is for operating point 2. In both cases, the GAPOD-based DC type of voltage regulator provides effective damping compared to conventional controllers.

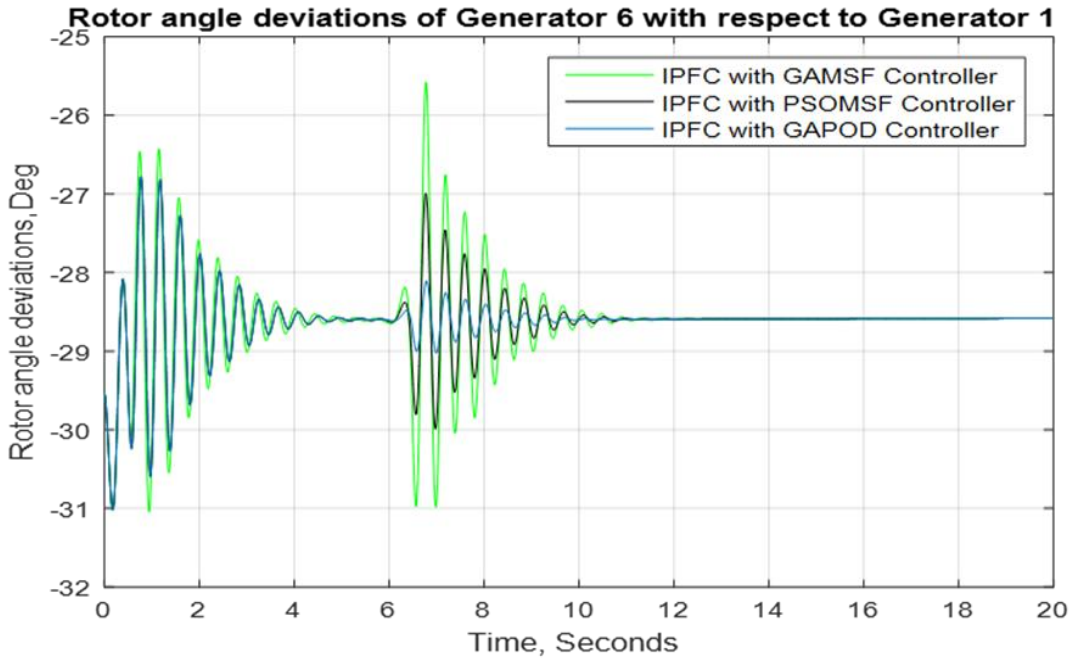

Fig. 9 TR of the deviation in the rotor's angle of machine no. 6 concerning machine or generator no.1 utilising the conventional/traditional type of controller, the GAMSF-based controller, the PSO-MSF-based DC type of voltage controller and the GAPOD-based DC type of voltage regulator at operating points 1 and 2 in the MMPS

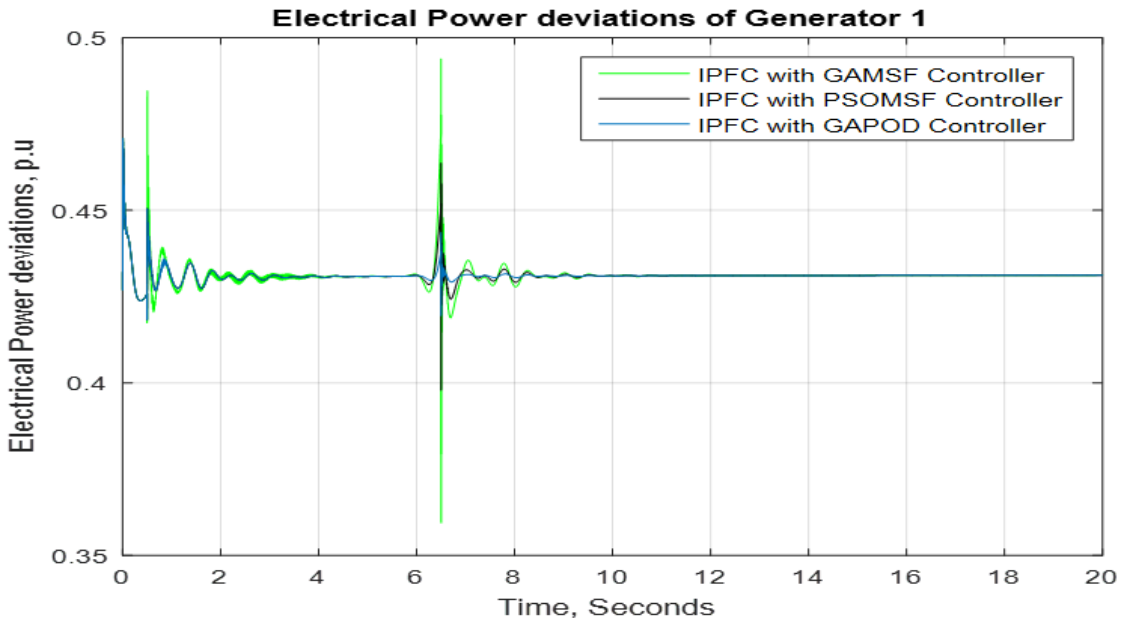

Fig. 10 TR of the electrical power deviations of the machine or generator no. 1 utilising the GAMSF-based DC type of voltage regulators, the PSO-MSF-based DC type of voltage controller and the GAPOD-based DC type of voltage regulator at operating points 1 and 2 in the MMPS.

Fig. 9 shows the time-responses of the deviation in the rotor's angle of machine no.6 concerning machine or generator no.1 using the conventional/traditional type of controller, the GAMSF-based controller, the PSO-MSF-based DC type of voltage controller and the GAPOD-based DC type of voltage regulator at the first and second points of operation in the MMPS. In the simulated results shown, the first part, from 0 to 6 seconds, is for operating point 1 and the second part, from 6 to 12 seconds, is for operating point 2. In both cases, the GAPOD-based DC type of voltage regulator provides effective damping compared to conventional controllers.

Fig. 10 shows the time-responses of the electrical power deviations of machine no.1 using the GAMSF-based DC type of voltage controller, the PSO-MSF-based DC type of voltage controller and the GAPOD-based DC type of voltage regulator at the first and second points of operation in the MMPS. In the simulated results shown, the first part, from 0 to 6 seconds, is for operating point 1 and the second part, from 6 to 12 seconds, is for operating point 2. In both cases, the GAPOD-based DC type of voltage regulator provides effective damping compared to conventional controllers.

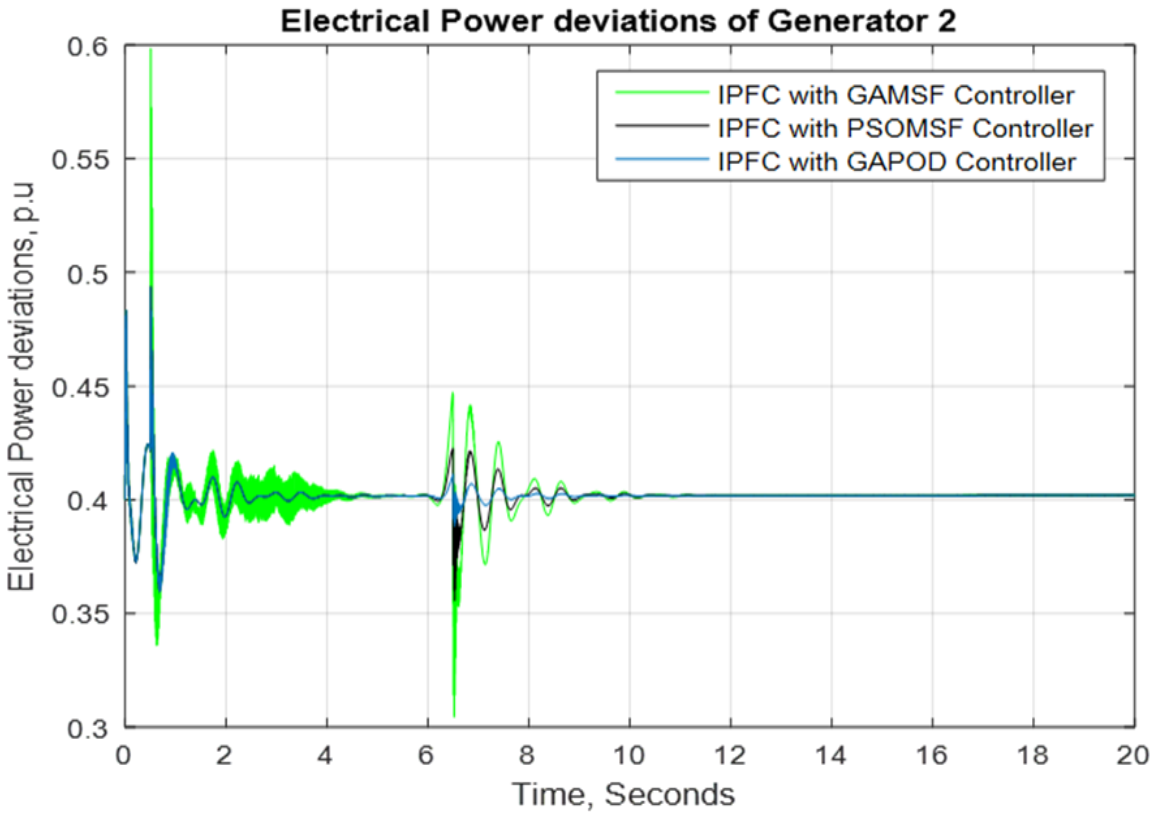

Fig. 11 TR of the electrical power deviations of machine or generator no. 2 utilising the GAMSF-based DC type of voltage regulators, the PSO-MSF-based DC type of voltage controller and the GAPOD-based DC type of voltage regulator at operating points 1 and 2 in the MMPS

Fig. 11 shows the time-responses of the electrical power deviations of machine no.2 using the GAMSF-based DC type of voltage controller, the PSO-MSF-based DC type of voltage controller and the GAPOD-based DC type of voltage regulator at the first and second points of operation in the MMPS. In the simulated results shown, the first part, from 0 to 6 seconds, is for operating point 1 and the second part, from 6 to 12 seconds, is for operating point 2. In both cases, the GAPOD-based DC type of voltage regulator provides effective damping compared to conventional controllers.

Fig. 12 shows the time-responses of the electrical power deviations of machine no. 4 using the GAMSF-based DC type of voltage controller, the PSO-MSF-based DC type of voltage controller and the GAPOD-based DC type of voltage regulator at the first and second points of operation in the MMPS. In the simulated results shown, the first part, from 0 to 6 seconds, is for operating point 1 and the second part, from 6 to 12 seconds, is for operating point 2. In both cases, the GAPOD-based DC type of voltage regulator provides effective damping compared to conventional controllers.

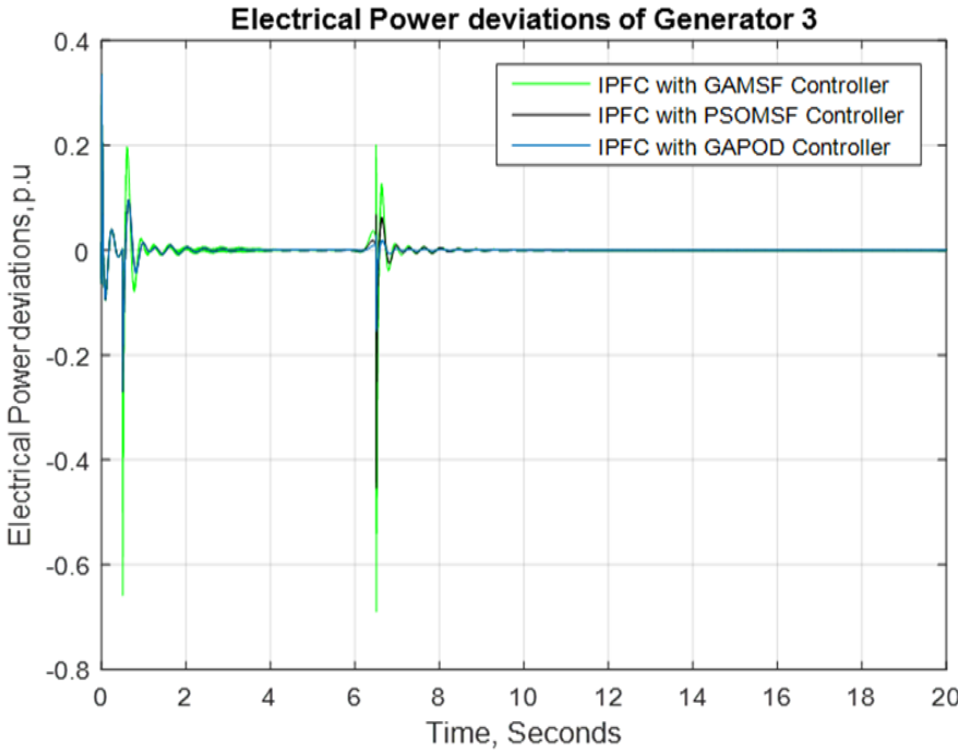

Fig. 12 TR of the electrical power deviations of the machine or generator no. 4 utilising the GAMSF-based DC type of voltage regulator, the PSO-MSF-based DC type of voltage controller and the GAPOD-based DC type of voltage regulator at operating points 1 and 2 in the MMPS

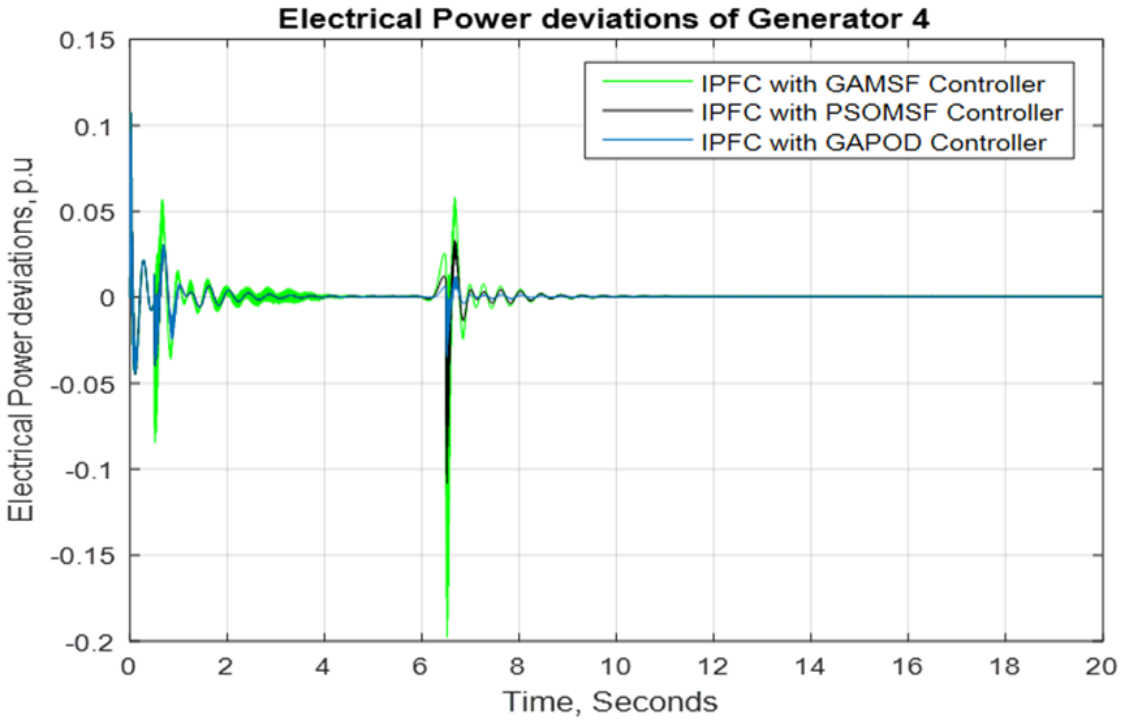

Fig. 13 TR of the electrical power deviations of the machine or generator no. 4 utilising the GAMSF-based DC type of voltage regulator, the PSO-MSF-based DC type of voltage controller and the GAPOD-based DC type of voltage regulator at operating points 1 and 2 in the MMPS

Fig. 13 shows the time-responses of the electrical power deviations of machine no.4 using the GAMSF-based DC type of voltage controller, the PSO-MSF-based DC type of voltage controller and the GAPOD-based DC type of voltage regulator at the first and second points of operation in the MMPS. In the simulated results shown, the first part, from 0 to 6 seconds, is for operating point 1, and the second part, from 6 to 12 seconds, is for operating point 2. In both cases, the GAPOD-based DC type of voltage regulator provides effective damping compared to conventional controllers.

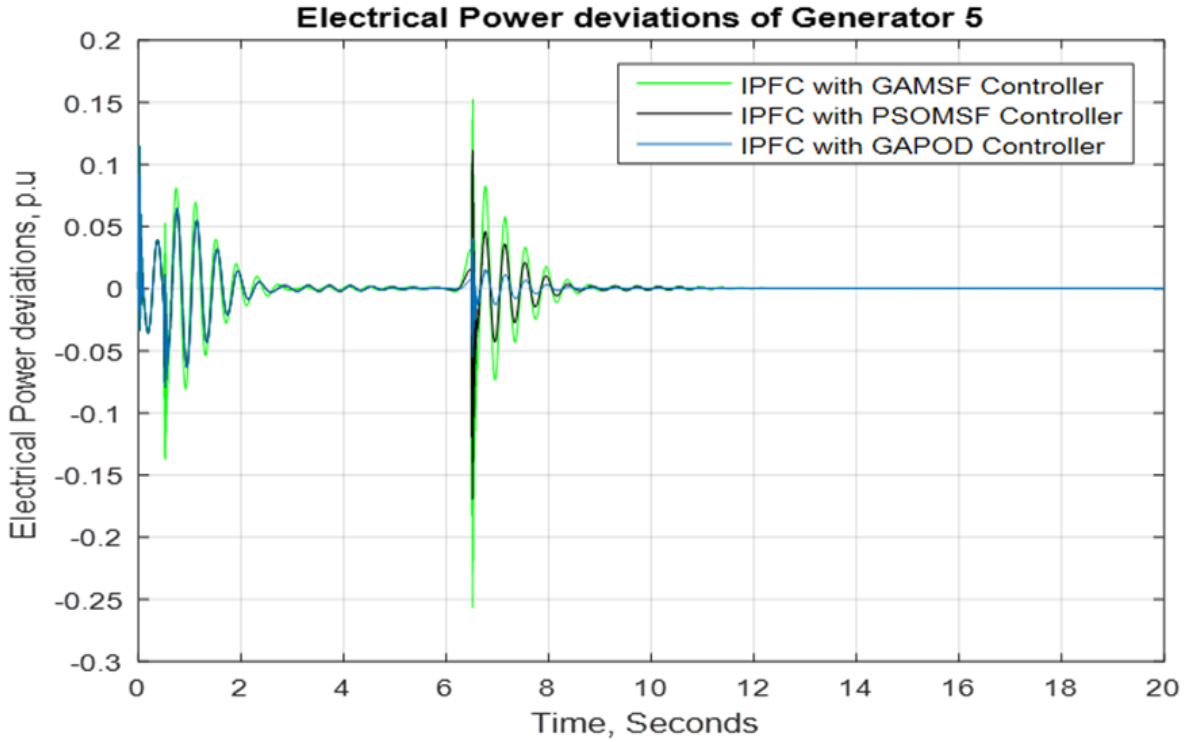

Fig. 14 TR of the electrical power deviations of the machine or generator no. 5 utilising the GAMSF-based DC type of voltage regulator, the PSO-MSF-based DC type of voltage controller and the GAPOD-based DC type of voltage regulator at operating points1 and 2 in the MMPS

Fig. 14 shows the time-responses of the electrical power deviations of machine no. 5 using the GAMSF-based DC type of voltage controller, PSO-MSF-based DC type of voltage controller, and the GAPOD-based DC type of voltage regulator at the first and second points of operation in the MMPS. In the simulated results shown, the first part from 0 to 6 seconds is for operating point 1, and the second from 6 to 12 seconds is for operating point 2. In both cases, the GAPOD-based DC type of voltage regulator provides effective damping compared to conventional controllers.

Fig. 15 shows the time-responses of the electrical power deviations of machine no.6 using the GAMSF-based DC type of voltage controller, the PSO-MSF-based DC type of voltage controller and the GAPOD-based DC type of voltage regulator at the first and second points of operation in the MMPS. In the simulated results shown, the first part, from 0 to 6 seconds, is for operating point 1 and the second part, from 6 to 12 seconds, is for operating point 2. In both cases, the GAPOD-based DC type of voltage regulator provides effective damping compared to conventional controllers.

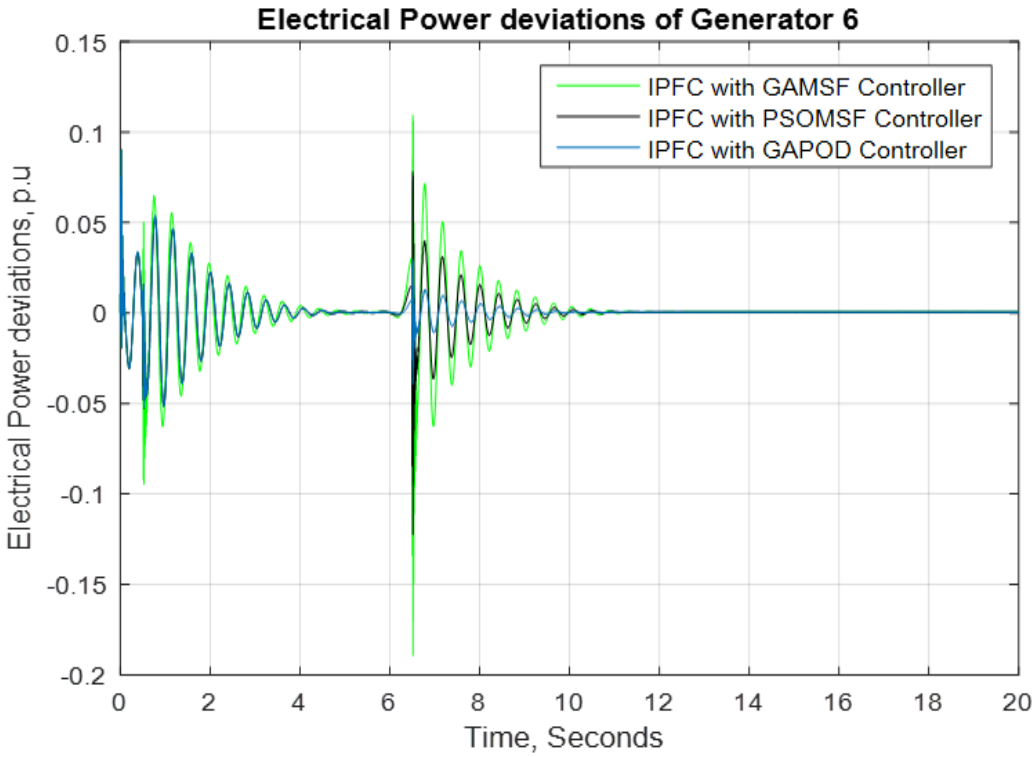

Fig. 15 TR of the electrical power deviations of the machine or generator no. 6 utilising the GAMSF-based DC type of voltage regulators, the PSO-MSF-based DC type of voltage controller and the GAPOD-based DC type of voltage regulator at operating points 1 and 2 in the MMPS

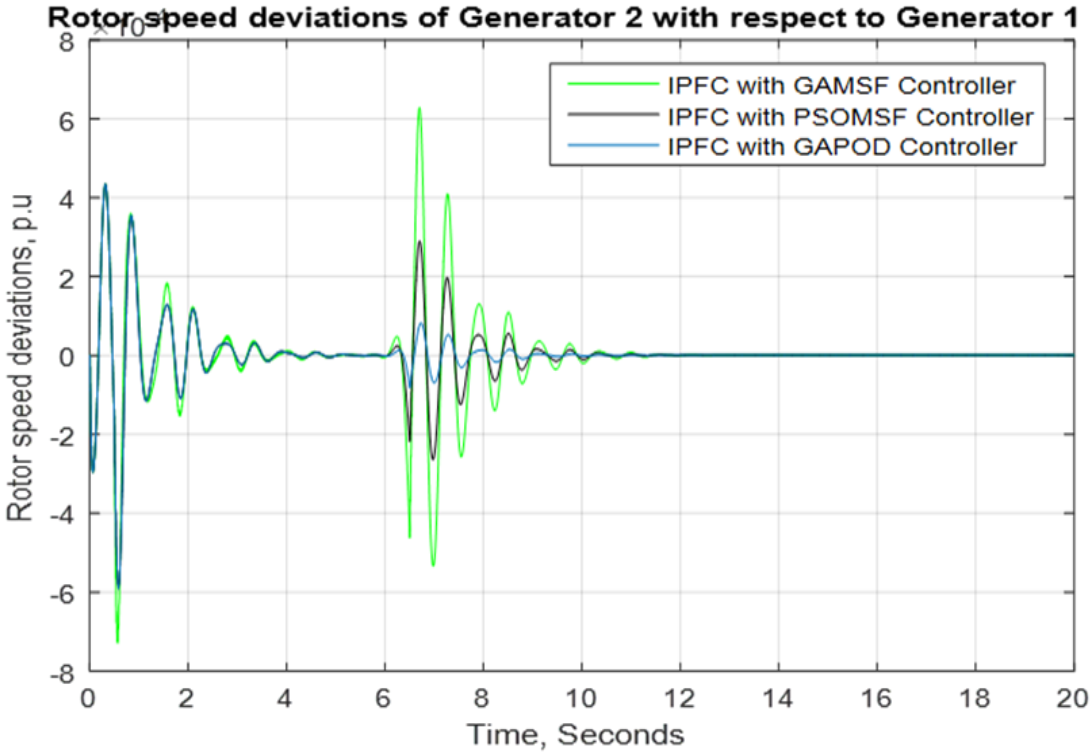

Fig. 16 TR of the deviation in the speed of the rotor of the machine or generator no. 2 concerning machine no.1 utilising the GAMSF-based DC type of voltage regulator, the PSO-MSF-based DC type of voltage controller and the GAPOD-based DC type of voltage regulator at operating points 1 and 2 in the MMPS

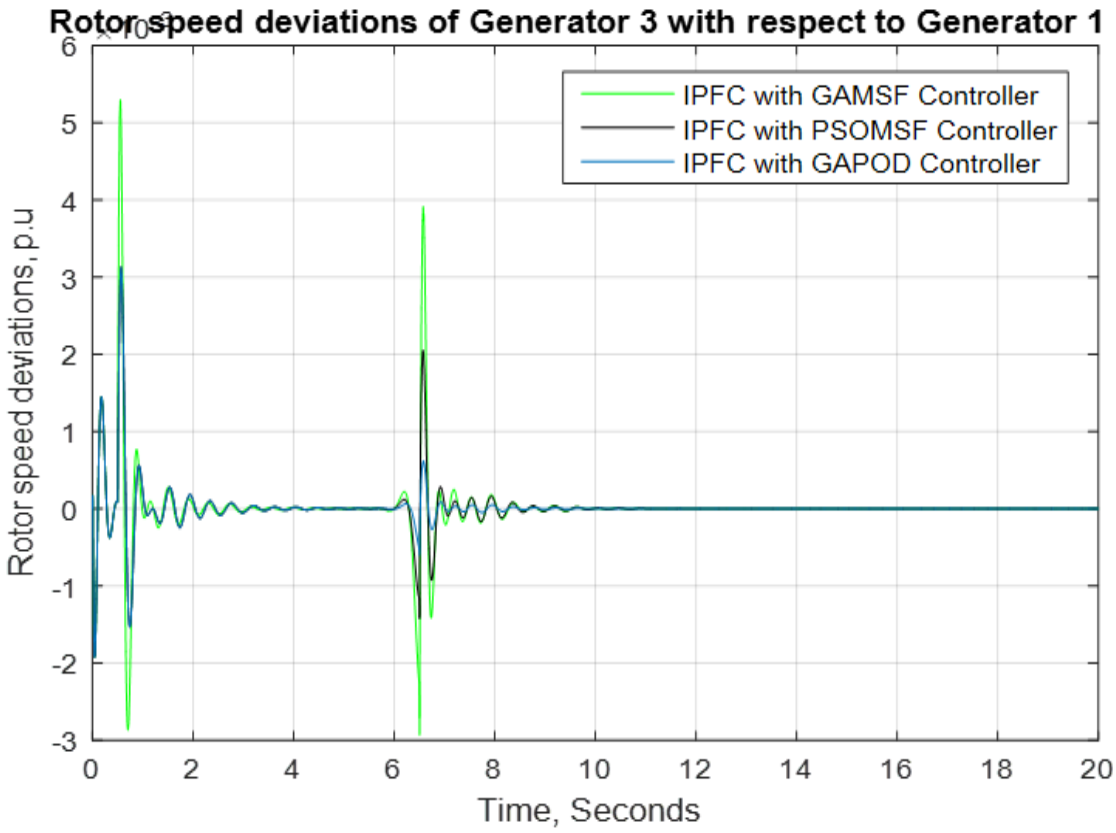

Fig. 17 TR of the deviation in the speed of the rotor of the machine or generator no.3 concerning machine no.1 utilising the GAMSF-based DC type of voltage regulator, the PSO-MSF-based DC type of voltage controller and the GAPOD-based DC type of voltage regulator at operating points 1 and 2 in the MMPS

Fig. 16 shows the time-responses of the deviation in the speed of the rotor of machine no.2 concerning machine no.1 using the GAMSF-based DC type of voltage controller, the PSO-MSF-based DC type of voltage controller and the GAPOD-based DC type of voltage controller at the first and second points of operation in the MMPS. In the simulated results shown, the first part, from 0 to 6 seconds, is for operating point 1 and the second part, from 6 to 12 seconds, is for operating point 2. In both cases, the GAPOD-based DC type of voltage regulator provides effective damping compared to conventional controllers.

Fig. 17 shows the time-responses of the deviation in the speed of the rotor of machine no.3 concerning machine no.1 using the GAMSF-based DC type of voltage controller, the PSO-MSF-based DC type of voltage controller and the GAPOD-based DC type of voltage controller at the first and second points of operation in the MMPS. In the simulated results shown, the first part, from 0 to 6 seconds, is for operating point 1 and the second part, from 6 to 12 seconds, is for operating point 2. In both cases, the GAPOD-based DC type of voltage regulator provides effective damping compared to conventional controllers.

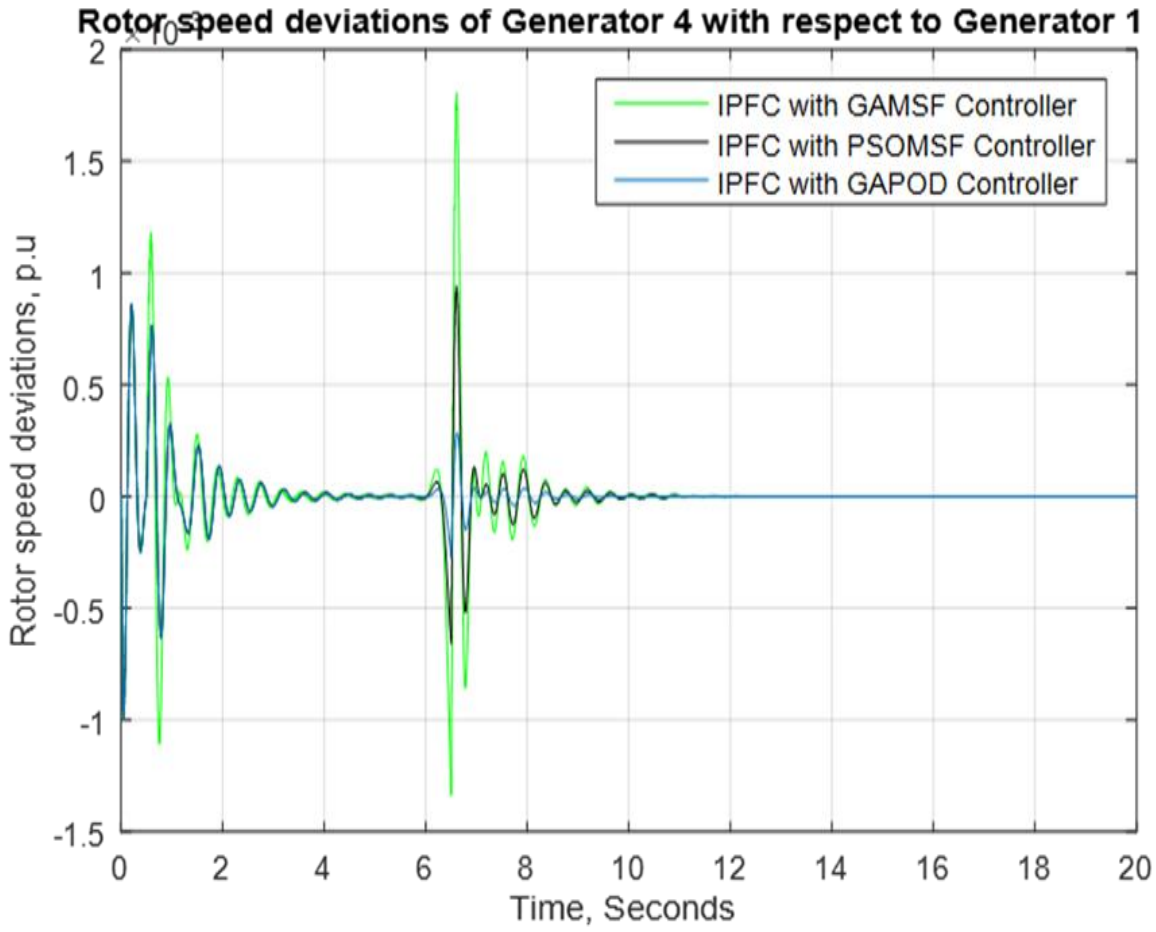

Fig. 18 TR of the deviation in the speed of the rotor of the machine or generator no. 4 concerning machine no. 1 utilising the GAMSF-based DC type of voltage regulator, the PSO-MSF-based DC type of voltage controller and the GAPOD-based DC type of voltage regulator at operating points 1 and 2 in the MMPS

Fig. 18 shows the time-responses of the deviation in the speed of the rotor of machine no. 4 concerning machine no.1 using the GAMSF-based DC type of voltage controller, the PSO-MSF-based DC type of voltage controller and the GAPOD-based DC type of voltage controller at the first and second points of operation in the MMPS. In the simulated results shown, the first part, from 0 to 6 seconds, is for operating point 1 and the second part, from 6 to 12 seconds, is for operating point 2. In both cases, the GAPOD-based DC type of voltage regulator provides effective damping compared to conventional controllers.

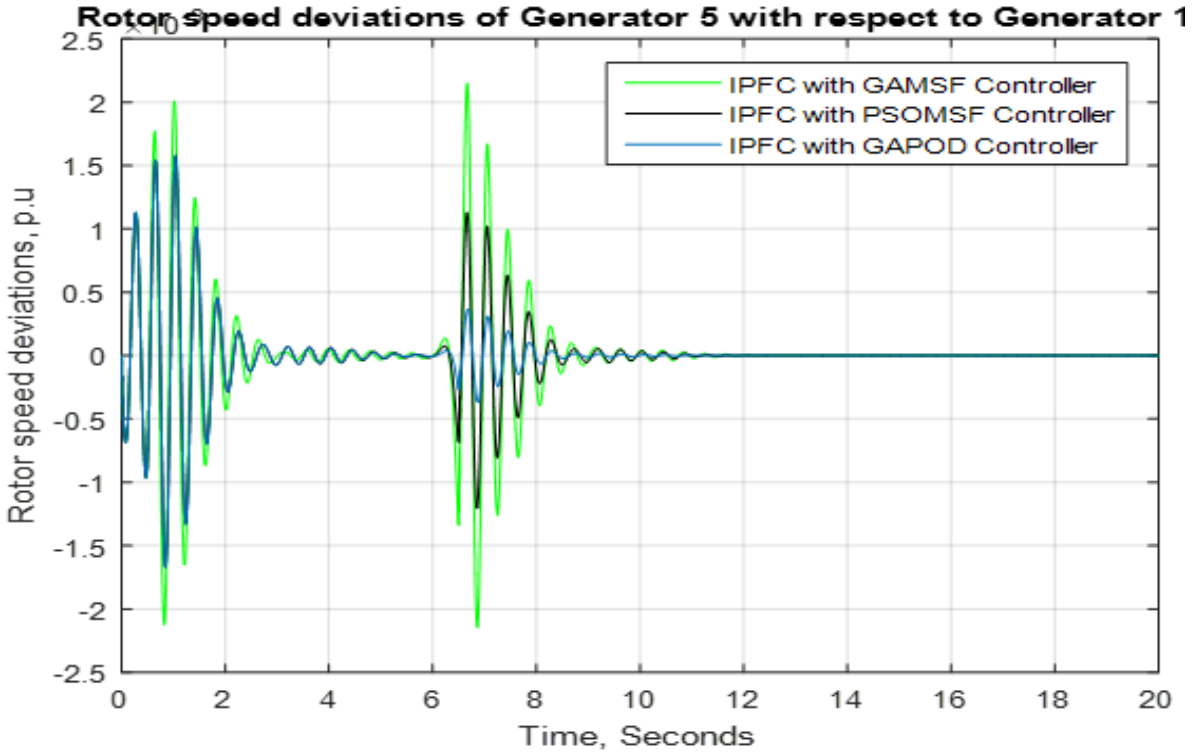

Fig. 19 TR of the deviation in the speed of the rotor of machine or generator no.5 concerning machine no.1 utilising the GAMSF-based DC type of voltage regulator, the PSO-MSF-based DC type of voltage controller and the GAPOD-based DC type of voltage regulator at operating points 1 and 2 in the MMPS

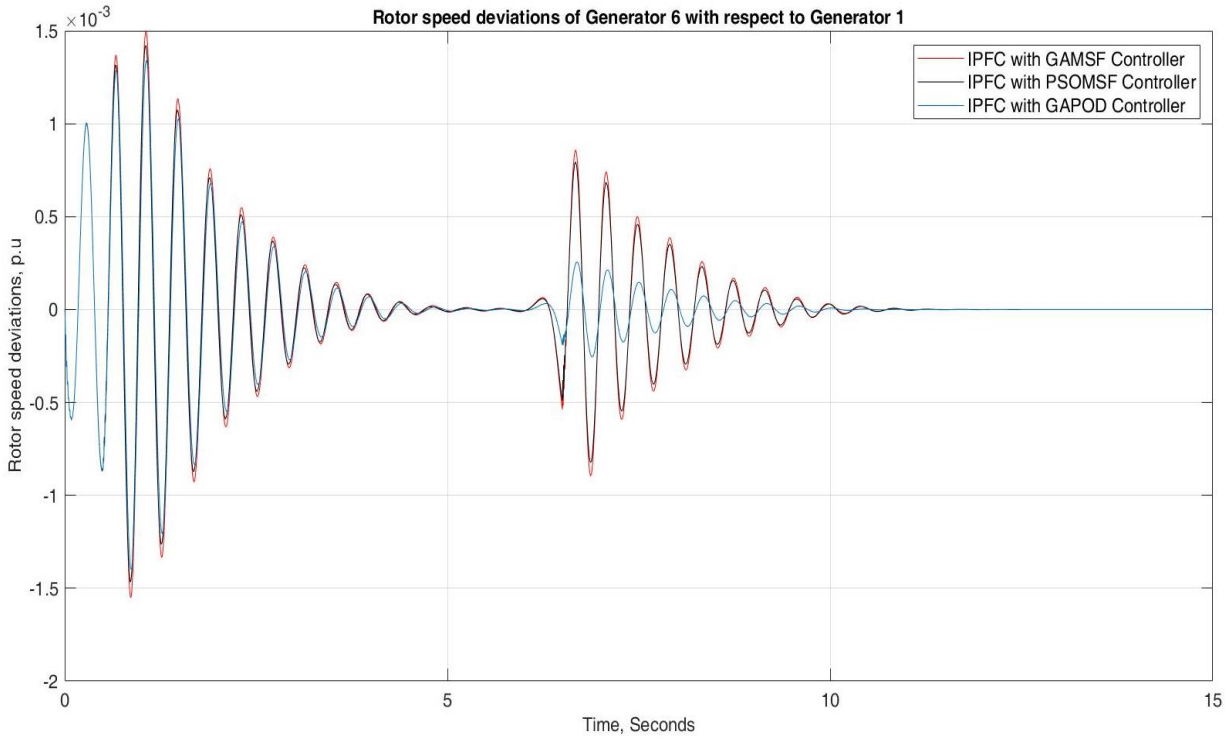

Fig. 20 TR of the deviation in the speed of the rotor of the machine or generator no. 6 concerning machine no.1 utilising the GAMSF-based DC type of voltage regulators, the PSO-MSF-based DC type of voltage controller and the GAPOD-based DC type of voltage regulator at operating points 1 and 2 in the MMPS

Fig. 19 shows the time-responses of the deviation in the speed of the rotor of machine no.5 concerning machine no.1 using the GAMSF-based DC type of voltage controller, the PSO-MSF-based DC type of voltage controller and the GAPOD-based DC type of voltage controller at the first and second points of operation in the MMPS. In the simulated results shown, the first part, from 0 to 6 seconds, is for operating point 1 and the second part, from 6 to 12 seconds, is for operating point 2. In both cases, the GAPOD-based DC type of voltage regulator provides effective damping compared to conventional controllers.

Fig. 20 shows the time-responses of the deviation in the speed of the rotor of machine no.6 concerning machine no.1 using the GAMSF-based DC type of voltage controller, the PSO-MSF-based DC type of voltage controller and the GAPOD-based DC type of voltage controller at the first and second points of operation in the MMPS. In the simulated results shown, the first part, from 0 to 6 seconds, is for operating point 1 and the second part, from 6 to 12 seconds, is for operating point 2.

Considering figures5–20, the simulation results indicated that the genetic algorithm-based DC type of voltage controller would provide more additional and improvised damping effects compared with the PSO-MSF-based DC type of voltage controller at different points of operations in their harmonic reduction process.

4. Conclusion

In this work, the developed controller was compared to conventional IPFC-based controllers, GAMSF-based DC type of voltage regulator, and PSO-MSF-based DC type of voltage regulator to work under various operating parameters on the standard IEEE 6-generator 30-bus system equipped with IPFC Power System Frameworks. When compared to other developed controllers, viz., PSOMSF-based DC type of voltage regulators, GAMSF-based DC type of voltage regulators, and the traditional IPFC controller, the proposed GAPOD controller with GADC-based voltage regulators showed quite promising results considering the improvised damping efficiency, reduced peak overshoot and the times of settling concerning different operating conditions.

References

[1] SepidehBahravar, Helia Sadat Hosseinian, Mohammad Esmaeil Nazari, Javad Olamaei, "Modeling and Coordinated Control of IPFC and SVC to Improve the Low-Frequency Oscillation Damping," *26th Iranian Conference on Electrical Engineering* (*ICEE2018*), *IEEE*, 2018.

[2] Alivelu M. Parimi, Irraivan Elamvazuthi and Nordin Saad, "Damping of Inter-Area Oscillations Using Interline Power Flow Controller Based Damping Controllers," *2nd IEEE International Conference on Power and Energy* (*PECon 08*), *IEEE*, Johor Baharu, 2008.

[3] Mohammed Osman Hassan, Ahmed Khaled Alhaj, "Analysis and Performance of Interline Power Flow Controller (IPFC) for Damping Low-Frequency Oscillations," *IJAERD-2018*, vol. 5, no. 10, 2018.

[4] M. R. Banaei, A. KamiInterline, "Power Flow Controller Based Damping Controllers for Damping Low-Frequency Oscillations", *Conference Paper*, 2016.

[5] Ms. S.M. Belwanshi, Dr. V.K. Chandrakar, Prof. S.N. Dhurvey, "Performance Evaluation of IPFC by Using Fuzzy Logic Based Controller for Damping of Power System Oscillations", *Fourth International Conference on Emerging Trends in Engineering & Technology, IEEE*, 2011.

[6] Naresh Acharya, Nadarajah Mithulananthan *et al*., "Facts about Flexible AC Transmission Systems (FACTS) Controllers: Practical Installations and Benefits", *AUPEC, Australia, School of Engineering*, vol. 2, no. 184, pp. 25-28, 2005.

[7] Iravani M.R, P.L. Dandeno, K.H. Nguyen, D. Zhu, and D. Maratukulam, "Applications of Static Phase Shifters in Power Systems", *IEEE Trans. Power Delivery*, vol. 9, no. 3, pp. 1600–1608, 1994.

[8] Chen X.R., N.C. Pahalawaththa, U.D. Annakkage, and C Kumble, "Controlled Series Compensation for Improving Stability of Multi-Machine Power Systems", *IEEE Proc. Gen. Trans. and Distrib*, vol. 142, no. 4, pp. 361–366, 1995.

[9] M.E. Aboul-Ela, A.A. Salam, J.D. McCalley and A.A. Fouad, "Damping Controller Design for Power System Oscillations Using Global Signals", *IEEE Transactions on Power Systems*, vol. 11, no. 2, pp. 767-773, 1996.

[10] Ch. Lokeshwar Reddy, P.Rajesh Kumar, "Study of Star Connected Cascaded H-Bridge STATCOM using Different PWM Techniques", *CVR Journal of Science and Technology*, vol. 13, pp. 61-66, 2017.

Authors' Information

Dr. D. Obulesu received his B.E. degree in Electrical and Electronics Engineering from STJ Institute of Technology, Karnataka University, India, in 2000 and his M. Tech in Power Electronics and Drives from Dr. M.G.R. University in 2005. He received his PhD in Electrical Engineering from JNTU, Hyderabad, India, in 2015. He has teaching experience of nearly 17 years. Currently, he is working as an Associate Professor at CVR College of Engineering, Telangana, India, in the Department of Electrical & Electronics Engineering. He has published a number of research papers in various national and international journals and conferences. His interests include neural networks, fuzzy logic, artificial intelligence, power electronics, MATLAB, FACTS, etc.

Dr. Manjunatha S C received his B.E. degree in Electrical & Electronics Engineering from Visvesvaraya Technological University, Belagavi, Karnataka, India, in 2008 and an M.Tech degree in Power System and Power Electronics from Kuvempu University Shivamogga, Karnataka, India in 2010. He received Ph.D. Degree from Visvesvaraya Technological University Belagavi, Karnataka, India, in 2021. He has teaching experience for nearly 12 years. Currently, he is working as Associate Professor in the department of EEE, SJMIT, Chitradurga, Karnataka, India. He has published a number of papers in national and international journals and has performed several projects.